Theory for Gas Solubility and Hydrophobic Interaction in Aqueous Electrolyte Solutions

Ryuichi Okamoto[a*] and Kenichiro Koga[a]

[a]Research Institute for Interdisciplinary Science, Okayama University, Okayama 700-8530, Japan

*E-mail: okamoto-ryuichi@okayama-u.ac.jp

Abstract

Ion specific effects on the solubility of nonpolar solutes and on the solute-solute hydrophobic interaction in aqueous electrolyte solutions are studied based on a continuum theory that incorporates the excluded volume of the molecules using the four-component (water, cations, anions, and solutes) Boublík-Mansoori-Carnahan-Starling-Leland model and the ion-hydration (electrostriction) using the Born model. We examine how the ordering of ions in the salt effect on the solubility as measured by the Sechenov coefficient K_S changes with varying sizes of ions and solutes. Our calculation reproduces the general trend of experimentally measured K_S and also provides an insight into the irregular behavior of K_S for lithium ion. The correlation between K_S and the salt effect on the hydrophobic interaction that has been pointed out earlier is accounted for by an explicit connection between K_S and the salt-enhanced-association coefficient C_I in the expansion of the second osmotic virial coefficient $B(n_s) = B(0) - C_I n_s + \cdots$ in powers of the salt density n_s at fixed pressure and temperature. The quadratic relation $C_I \approx K_S^2/4$ is derived for ions and solutes that are not very large.

Introduction

Specific ion effects have been a long-standing problem in properties of aqueous solutions of electrolytes such as salt activity coefficient,[1,2]

surface tension,[3,4] viscosity,[5] and nanobubble stability[6] in aqueous electrolyte solutions. Addition of ions to a fluid mixture can induce phase separation, and whether macroscale or microscale separation occurs depends on the salt species.[7–10] Ion-specificity is often referred to as the Hofmeister effect, which, in the original sense, is the ion-specificity of the ability for salting-out/salting-in proteins.[11] Contrary to the initial expectation that the (original) Hofmeister effect is determined by the bulk properties of aqueous electrolyte solutions, researches in the last decades indicate that it is in fact a result of complex interplays of specific interactions among ions, water, and hydrophilic/hydrophobic groups of proteins.[12,13]

Ion-specificity in the solubility of simple nonionic solutes (gasses) in aqueous electrolyte solutions has also been known for long, since Sechenov (Setschenow) empirically found the relation[14] $-\ln \Sigma \approx K_S n_s$ between the Ostwald adsorption coefficient Σ and the salt density n_s. The proportionality coefficient K_S, which is usually positive (salting-out), is now called the Sechenov coefficient, and is specific to both ion and solute species. Its experimental data are available for many combination of ions and solutes.[15–19] Molecular dynamics (MD) simulations,[20–23] molecular-based theory,[24] and Monte-carlo (MC) simulation[25] have reproduced some of the data including a notable irregular behavior of Li^{+}. The Sechenov coefficient K_S usually increases as the ion (resp. solute) size becomes smaller (resp. larger),

whereas for some large ions it decreases as the solute size becomes larger and can even be negative (salting-in). Early theoretical studies[15,26] have provided simple explanation for some of these features, but overall understanding has yet to be completed.

The Sechenov coefficient K_S is a measure of the specific ion effect on the solvation free energy μ_h^* of an isolated, single solute molecule in a solvent; it is *not* a direct measure of the ion effect on the solute-solute effective interaction in the solvent. In the present study, we introduce a new measure C_I for the ion effect on the solute-solute effective interaction and evaluate in terms of C_I the specific ion effects on the hydrophobic interaction.

The effective pair interaction between solute molecules is expressed as the solute-solute potential of mean force (PMF). Using MD[27-29] and MC[30] simulations, some authors found that an addition of salt leads to a downward shift of the solute-solute PMF. Furthermore, Thomas and Elcock[31] found that the magnitude of the shift is greater for ions with larger K_S. Another measure of the solute-solute effective interaction is the second osmotic virial coefficient $B = -G_{hh}^0/2$, where G_{hh}^0 is the solute-solute Kirkwood-Buff integral[32] in the dilute limit. Recently, Koga and Yamamoto[33] performed MD simulations of a methane-NaCl-water solution, and found a similar correlation between μ_h^* and B as the salt concentration is varied. The understanding of the ion- and solute-specificity in these correlations, however, remains qualitative.

The following thermodynamic identity for B was derived in an earlier study of binary (solvent+solute) solutions:[34,35]

$$B = B'' - (v_h - k_B T \kappa_w)^2/2k_B T \kappa_w, \quad (1)$$

where B'' is the coefficient analogous to B in the expansion of the osmotic pressure with respect to the solute density n_h at fixed density n_w of the solvent, instead of fixed chemical potential of the solvent. Equivalently, B'' appears as a coefficient in the expansion of the solute excess chemical potential μ_h^* with respect to n_h as $B'' = (1/2k_B T) \lim_{n_h \to 0}(\partial \mu_h^*/\partial n_h)_{T,n_w}$. In

the second term of (1), v_h is the solute partial molecular volume in the dilute limit, and κ_w the isothermal compressibility of pure solvent. It was recently noted that B'' is given by the integral of the solute-solute direct correlation function,[2]

$$B'' = -\frac{1}{2} \int c_{hh}(\boldsymbol{r})d\boldsymbol{r} \qquad (n_h \to 0), \quad (2)$$

which is in correspondence with the Kirkwood-Buff expression for B

$$B = -\frac{1}{2} \int h_{hh}(\boldsymbol{r})d\boldsymbol{r} \qquad (n_h \to 0), \quad (3)$$

where h_{hh} is the solute-solute pair correlation function.

While the second term of Eq. (1) is considerably negative, B'' is usually positive, and hence B can be either positive (repulsive) or negative (attractive). Combining the identity (1) and van der Waals-type equations of state, Cerdeiriña and Widom calculated B as well as the contributions to it, B'' and $B - B''$, and discussed their temperature dependencies.[35] More recently, it has been found that extensions of Eq. (1) naturally appear in studying density fluctuations and thermodynamic behaviors of ternary non-ionic fluids (binary solvent + solute)[36] and of aqueous electrolyte solutions.[2] In the former work, a new term due to the solvent composition fluctuations is added to Eq. (1), and can be a dominant factor of solute-solute effective interaction. In the latter, counterparts of the second term of Eq. (1) have played essential roles in ion-size-dependence of the activity and osmotic coefficients.

In this paper, we develop a continuum theory for the gas solubility and the solute-solute effective interaction in aqueous electrolyte solutions; we shall find K_S and B can be expressed as the generalizations of Eq. (1). Combining the Boublík-Mansoori-Carnahan-Starling-Leland (BMCSL) model[37,38] and the Born model,[39] we investigate the Sechenov coefficient K_S and the coefficient C_I introduced in Eq. (40), which are, respectively, measures of the salt effects on the solubility of solutes and the solute-solute interaction. More specifically, we exam-

ine the ion-size and the solute-size dependencies of K_S and C_I.

The organization of this paper is as follows. We start with a review of thermodynamic quantities of fluid mixtures, e.g., isothermal compressibility and partial volumes. We then derive expressions for the Sechenov coefficient and the second osmotic virial coefficient of the solutes. The partial volumes of individual ion species are also introduced; they can neither be defined in thermodynamics nor measured in experiments, but are convenient in understanding the numerical analysis. We then introduce a simple model for liquid solutions composed of solvent (water), salt, and solute. We use the BMCSL model for the steric effects and the Born model for ion-hydration (electrostriction). We then numerically examine the ion-size- and solute-size-dependence of K_S and C_I, as well as the correlation between them. Final section is devoted for summary and remarks.

Theory

For simplicity we consider 1:1 salt, which in water dissociates into cations and anions of electric charges e and $-e$, respectively. Let $\hat{n}_\mathrm{w}$, $\hat{n}_\mathrm{c}$, $\hat{n}_\mathrm{a}$, and $\hat{n}_\mathrm{h}$ denote the fluctuating number densities of water, cation, anion, and hydrophobic solute (gas), respectively. In equilibrium, their average values are homogeneous in space. The average water and solute densities are denoted by n_w and n_h,

$$\langle \hat{n}_\mathrm{w} \rangle = n_\mathrm{w}, \quad \langle \hat{n}_\mathrm{h} \rangle = n_\mathrm{h}, \tag{4}$$

and the average ion densities satisfy the charge neutrality condition,

$$\langle \hat{n}_\mathrm{c} \rangle = \langle \hat{n}_\mathrm{a} \rangle = n_\mathrm{s} = n_\mathrm{I}/2. \tag{5}$$

Here n_s is the salt density, and n_I the total ion density. Throughout the paper, we shall study solubility and interaction of the *almost infinitely-dilute* hydrophobic solute in a *dilute* electrolyte solution (solvent). That is, we assume

$$n_\mathrm{h} \ll n_\mathrm{I} \ll n_\mathrm{w}. \tag{6}$$

In the following, we shall not take the limit $n_\mathrm{I} \to 0$ unless the limit $n_\mathrm{h} \to 0$ is taken in advance.

Thermodynamics

We can generally expand the Helmholtz free energy density $f(n_\mathrm{w}, n_\mathrm{I}, n_\mathrm{h})$ in powers of n_h,

$$\begin{aligned} f =& f^\mathrm{s}(n_\mathrm{w}, n_\mathrm{I}) + k_\mathrm{B}T n_\mathrm{h}\{\ln(n_\mathrm{h}\lambda_\mathrm{h}^3) - 1\} \\ &+ k_\mathrm{B}T n_\mathrm{h}\nu_\mathrm{h}^\mathrm{s}(n_\mathrm{w}, n_\mathrm{I}) + \frac{n_\mathrm{h}^2}{2}U_\mathrm{hh}^\mathrm{s}(n_\mathrm{w}, n_\mathrm{I}) + \cdots, \end{aligned} \tag{7}$$

where the logarithmic term, which is singular at $n_\mathrm{h} = 0$, has not been expanded. In the above λ_h is the thermal de Broglie length of the solute, f^s the Helmholtz free energy density of the electrolyte solution without the solute, $k_\mathrm{B}T\nu_\mathrm{h}^\mathrm{s} = \mu_\mathrm{h}^*$ the solvation free energy or excess chemical potential of the solute at infinite dilution ($n_\mathrm{h} = 0$), and the coefficient U_hh^s of n_h^2 is the contribution arising from the solute-solute interaction.

The chemical potentials μ_i ($i = \mathrm{w}, \mathrm{I}, \mathrm{h}$) and the pressure p are expressed in terms of f as

$$\mu_i = \partial f/\partial n_i \tag{8}$$

$$p = \sum_{j=\mathrm{w,I,h}} n_j(\partial f/\partial n_j) - f. \tag{9}$$

Hereafter the quantities are regarded as functions of the temperature T and the densities $\{n_i\}$, and hence the partial derivatives with respect to n_i are taken with fixed T and $\{n_j\}_{j \neq i}$, unless otherwise indicated explicitly (e.g., Eq. (25)). Using Eq. (9), the isothermal compressibility $\kappa_T = -V^{-1}(\partial V/\partial p)_{T,\{N_j\}}$ is expressed as

$$\kappa_T^{-1} = k_\mathrm{B}T \sum_{i,j=\mathrm{w,I,h}} n_i n_j I^{ij}, \tag{10}$$

with the second derivatives,

$$k_\mathrm{B}T I^{ij} \equiv \partial^2 f/\partial n_i \partial n_j = (\partial \mu_i/\partial n_j)_{T,\{n_k\}_{k \neq j}}. \tag{11}$$

In particular, the isothermal compressibility for

pure water κ_{w} is given by

$$\kappa_{\mathrm{w}}^{-1} = n_{\mathrm{w}}^2 (\partial^2 f_{\mathrm{w}}/\partial n_{\mathrm{w}}^2) = k_{\mathrm{B}} T n_{\mathrm{w}}^2 \lim_{n_{\mathrm{I}}, n_{\mathrm{h}} \to 0} I^{\mathrm{ww}}, \tag{12}$$

where $f_{\mathrm{w}}(n_{\mathrm{w}}) = f^{\mathrm{s}}(n_{\mathrm{w}}, 0)$ is the Helmholtz free energy density of pure water.

We also define the (dimensionless) excess chemical potential of the solute ν_{h} in pure water and the ion-solute direct interaction coefficient U_{hI} in water as

$$\nu_{\mathrm{h}}(n_{\mathrm{w}}) \equiv \nu_{\mathrm{h}}^{\mathrm{s}}(n_{\mathrm{w}}, 0) \tag{13}$$

$$U_{\mathrm{hI}} \equiv k_{\mathrm{B}} T \lim_{n_{\mathrm{I}} \to 0} (\partial \nu_{\mathrm{h}}^{\mathrm{s}}/\partial n_{\mathrm{I}}) = k_{\mathrm{B}} T \lim_{n_{\mathrm{I}}, n_{\mathrm{h}} \to 0} I^{\mathrm{hI}}. \tag{14}$$

Partial volumes

Let V and N_i denote the system volume and the particle number of species i $(= \mathrm{w}, \mathrm{I}, \mathrm{h})$, respectively. The partial molecular volume of species i is defined as $\bar{v}_i = (\partial V/\partial N_i)_{T, p, \{N_j\}_{j \neq i}}$. Note that in the previous paper[2] the salt partial volume $\bar{v}_{\mathrm{s}} = (\partial V/\partial (N_{\mathrm{I}}/2))_{T, p, \{N_j\}_{j \neq \mathrm{I}}} = 2\bar{v}_{\mathrm{I}}$ was discussed instead of $\bar{v}_{\mathrm{I}}$. From the definition of $\bar{v}_i$, we derive

$$\bar{v}_i = \kappa_T (\partial p/\partial n_i)_{T, \{n_j\}_{j \neq i}} = k_{\mathrm{B}} T \kappa_T \sum_{j=\mathrm{w}, \mathrm{I}, \mathrm{h}} I^{ij} n_j, \tag{15}$$

where we have used Eq. (9) in the second equality. The solvation partial volume is also defined as

$$\bar{v}_i^* \equiv \bar{v}_i - k_{\mathrm{B}} T \kappa_T. \tag{16}$$

For nearly incompressible solvent such as aqueous electrolyte solutions, these two partial volumes almost coincide, $v_i^{\mathrm{s}*} \approx v_i^{\mathrm{s}}$ unless the molecular size of species i is too small. Since V and N_i are extensive variables, we have the sum rule,

$$\sum_{i=\mathrm{w}, \mathrm{I}, \mathrm{h}} n_i \bar{v}_i = 1. \tag{17}$$

For convenience, we shall introduce some symbols representing partial volumes in limiting cases. The partial volumes in the limit

$n_{\mathrm{h}} \to 0$ are written as v_i^{s} and $v_i^{\mathrm{s}*}$ $(i = \mathrm{w}, \mathrm{I}, \mathrm{h})$, i.e.,

$$v_i^{\mathrm{s}} \equiv \lim_{n_{\mathrm{h}} \to 0} \bar{v}_i, \quad v_i^{\mathrm{s}*} \equiv \lim_{n_{\mathrm{h}} \to 0} \bar{v}_i^* = v_i^{\mathrm{s}} - k_{\mathrm{B}} T \kappa_T^{\mathrm{s}}, \tag{18}$$

where $\kappa_T^{\mathrm{s}} = \lim_{n_{\mathrm{h}} \to 0} \kappa_T$ is the isothermal compressibility of the electrolyte solvent. Furthermore, let v_i and v_i^* denote the partial volumes in the limit, $n_{\mathrm{I}}, n_{\mathrm{h}} \to 0$:

$$v_i \equiv \lim_{n_{\mathrm{I}} \to 0} v_i^{\mathrm{s}}, \quad v_i^* \equiv \lim_{n_{\mathrm{I}} \to 0} v_i^{\mathrm{s}*} = v_i - k_{\mathrm{B}} T \kappa_{\mathrm{w}}. \tag{19}$$

Using Eq. (15) with Eqs. (7) and (11) and taking the limit $n_{\mathrm{h}} \to 0$, we have

$$v_{\mathrm{h}}^{\mathrm{s}} = k_{\mathrm{B}} T \kappa_T^{\mathrm{s}} \left[1 + \sum_{i=\mathrm{w}, \mathrm{I}} n_i (\partial \nu_{\mathrm{h}}^{\mathrm{s}}/\partial n_i) \right] \tag{20}$$

$$v_{\mathrm{h}}^{\mathrm{s}*} = k_{\mathrm{B}} T \kappa_T^{\mathrm{s}} \sum_{i=\mathrm{w}, \mathrm{I}} n_i (\partial \nu_{\mathrm{h}}^{\mathrm{s}}/\partial n_i). \tag{21}$$

In the limit $n_{\mathrm{I}} \to 0$, these reduce to

$$v_{\mathrm{h}} = k_{\mathrm{B}} T \kappa_{\mathrm{w}} (1 + n_{\mathrm{w}} \nu_{\mathrm{h}}'), \quad v_{\mathrm{h}}^* = k_{\mathrm{B}} T \kappa_{\mathrm{w}} n_{\mathrm{w}} \nu_{\mathrm{h}}', \tag{22}$$

where $\nu_{\mathrm{h}}' = \partial \nu_{\mathrm{h}}/\partial n_{\mathrm{w}}$. Without the ions and the solute, $n_{\mathrm{I}} = n_{\mathrm{h}} = 0$, Eq. (17) yields the trivial relation,

$$v_{\mathrm{w}} = 1/n_{\mathrm{w}}. \tag{23}$$

Isobaric condition and solvent composition susceptibility for $n_{\mathrm{h}} \to 0$

In this subsection, we assume the solute density is infinitely small, $n_{\mathrm{h}} \to 0$. In experiments, the pressure p is kept fixed as the salt density is varied (isobaric condition). This condition is written as

$$p(n_{\mathrm{w}}, n_{\mathrm{I}}) = p(n_{\mathrm{w}}^0, 0), \tag{24}$$

where n_{w}^0 is the water density without the salt. Differentiating Eq. (24) with respect to n_{I} and using Eq. (15), we obtain[2]

$$(\partial n_{\mathrm{w}}/\partial n_{\mathrm{I}})_{T, p} = -v_{\mathrm{I}}^{\mathrm{s}}/v_{\mathrm{w}}^{\mathrm{s}}. \tag{25}$$

4

The solvent particle density n and the ion molar fraction X_I are given by

$$n = n_w + n_I, \quad X_I = n_I/n. \qquad (26)$$

We define the composition susceptibility of the electrolyte solvent as $\chi_I \equiv k_B T n^{-1}(\partial X_I/\partial h)_{T,p}$ with $h = \mu_I - \mu_w$. Using Eq. (SI-13) in Supporting Information, we obtain

$$\chi_I^{-1} = n^3 \left[I_s^{ww} v_I^s + I_s^{II} v_w^s - I_s^{wI}(v_w^s + v_I^s) \right], \qquad (27)$$

where $I_s^{ij} = \lim_{n_h \to 0} I^{ij}$ $(i, j = w, I)$. The composition susceptibility χ_I is also a measure of the fluctuations of the total ion density $\hat{n}_c + \hat{n}_a$ in the long-wavelength limit [See Eq. (SI-37) in SI-D]. Because of the logarithmic term in Eq. (7), we have $I_s^{II} = 1/n_I + O(n_I^{-1/2})$ and $v_w^s = 1/n_w + O(n_I)$ as $n_I \to 0$. We hence have

$$\chi_I = n_I/n_w^2 + O(n_I^{3/2}). \qquad (28)$$

See Eq. (SI-49) for higher order contributions. We introduce the inverse matrix $\{I_{ij}^s\}_{i,j=w,I}$ of $\{I_s^{ij}\}_{i,j=w,I}$, and define $\Delta_0 = \det\{I_{ij}^s\} = [\det\{I_s^{ij}\}]^{-1}$. Using Eq. (15) and (10), we can rewrite Eq. (27) as[36]

$$\begin{aligned}
\chi_I &= \Delta_0/(k_B T n^4 \kappa_T^s) \\
&= n^{-4}(I_{ww}^s n_I^2 + I_{II}^s n_w^2 - 2I_{wI}^s n_w n_I). \qquad (29)
\end{aligned}$$

Sechenov coefficient

When the solution is in equilibrium with a gas phase, the solubility of a solute is measured by the Ostwald adsorption coefficient, i.e., the ratio of the solute density n_h in the solution to that in the gas phase n_h^{gas},

$$\Sigma = \lim_{n_h \to 0}(n_h/n_h^{gas}) = e^{-\nu_h^s}. \qquad (30)$$

The salting-out (salting-in) effect on the gas solubility in a dilute electrolyte solvent is measured by the Sechenov (Setschenow) coefficient,[14]

$$\begin{aligned}
K_S &= -\lim_{n_s \to 0} \left(\frac{\partial \ln \Sigma}{\partial n_s}\right)_{T,p} = 2 \lim_{n_I \to 0} \left(\frac{\partial \nu_h^s}{\partial n_I}\right)_{T,p} \\
&= (2/k_B T)(U_{hI} - v_h^* v_I/\kappa_w), \qquad (31)
\end{aligned}$$

where use has been made of Eqs. (14), (22), and (25) in the second line. In the literature, the Sechenov coefficient is often defined by $k_{scc} = -\lim_{n_s \to 0}(\partial \log_{10} \Sigma/\partial n_s)_{T,p} = K_S/\ln 10$, but in Eq. (31) we use natural logarithm as in the original work by Sechenov.[14] In analogy with Eq. (1), we introduce the effective solute-ion interaction coefficient as

$$U_{hI}^{eff} \equiv U_{hI} - v_h^* v_I^*/\kappa_w. \qquad (32)$$

We can then rewrite Eq. (31) as

$$K_S = (2/k_B T)(U_{hI}^{eff} - k_B T v_h^*). \qquad (33)$$

For general n_I, the Sechenov coefficient can be generalized to the solvation coefficient $g_h \equiv (\partial \nu_h^s/\partial X_I)_{T,p}$. This measures the *asymmetry* between the solute-water and solute-salt interactions. We can calculate this derivative using Eq. (SI-13):

$$g_h \equiv (\partial \nu_h^s/\partial X_I)_{T,p} = n^2 \left[v_w^s \frac{\partial \nu_h^s}{\partial n_I} - v_I^s \frac{\partial \nu_h^s}{\partial n_w} \right]. \qquad (34)$$

In the limit $n_I \to 0$, $\partial \nu_h^s/\partial n_I = U_{hI}/k_B T$ by definition (14) and $\partial \nu_h^s/\partial n_w \to v_h^*/k_B T n_w \kappa_w$ from (22), and so we have

$$\lim_{n_I \to 0} g_h = \frac{n_w}{k_B T}(U_{hI} - v_h^* v_I/\kappa_w) = n_w K_S/2, \qquad (35)$$

where the second equality follows from Eq. (31).

Second osmotic virial coefficient and salt-enhanced-association coefficient

Suppose a solution (water+ions+solute) and a solvent reservoir (water+ions) are separated by a semipermeable membrane that permeates only the water and ions. The chemical potentials of water μ_w and of ions μ_I are common in both regions, i.e., $\mu_i(n_w, n_I, n_h) = \mu_i(n_w^r, n_I^r, 0)$ for $i = $w, I, where n_w^r and n_I^r are the water and ion densities, respectively, in the reservoir. The osmotic pressure is the pressure difference between the two regions, $\Pi = p(n_w, n_I, n_h) - p(n_w^r, n_I^r, 0)$. In the expansion $\Pi = k_B T(n_h + B n_h^2 + \cdots)$, B is called the second osmotic virial

coefficient, which measures the effective solute-solute interaction.

We have the thermodynamic identities for elements of the inverse matrix $\{I_{ij}\}$ of $\{I^{ij}\}$ defined in Eq. (11):

$$I_{ij} = k_{\mathrm{B}}T(\partial n_i/\partial \mu_j)_{T,\{\mu_k\}_{k\neq j}} \quad (i,j=\mathrm{w},\mathrm{I},\mathrm{h}) \tag{36}$$

Note that as $n_{\mathrm{h}} \to 0$, the component $I^{\mathrm{hh}} \sim n_{\mathrm{h}}^{-1}$ diverges, but $\{I_{ij}\}_{i,j=\mathrm{w},\mathrm{I},\mathrm{h}}$ has a well-defined limit; in particular, for $i,j = \mathrm{w},\mathrm{I}$, the limit is equal to I_{ij}^{s} which has been defined above Eq. (29). See SI-A for detailed discussions.

As n_{h} is varied, the change rate of Π is $d\Pi/dn_{\mathrm{h}} = (\partial p/\partial n_{\mathrm{h}})_{T,\mu_{\mathrm{w}},\mu_{\mathrm{I}}} = k_{\mathrm{B}}Tn_{\mathrm{h}}/I_{\mathrm{hh}}$, where in the second equality we have used Gibbs-Duhem relation. We thus have

$$2B = \lim_{n_{\mathrm{h}}\to 0}(1/I_{\mathrm{hh}} - 1/n_{\mathrm{h}}). \tag{37}$$

From Eqs (37) and (SI-12), we obtain

$$B = U_{\mathrm{hh}}^{\mathrm{eff}}/2k_{\mathrm{B}}T. \tag{38}$$

where the effective solute-solute interaction coefficient $U_{\mathrm{hh}}^{\mathrm{eff}}$ is defined as

$$U_{\mathrm{hh}}^{\mathrm{eff}} \equiv U_{\mathrm{hh}}^{\mathrm{s}} - (v_{\mathrm{h}}^{\mathrm{s*}})^2/\kappa_T^{\mathrm{s}} - k_{\mathrm{B}}T\chi_{\mathrm{I}}g_{\mathrm{h}}^2. \tag{39}$$

with χ_{I} defined above Eq. (27) and g_{h} in Eq. (34). The coefficient $U_{\mathrm{hh}}^{\mathrm{eff}}$ is also a measure of the solute density fluctuations in the long-wavelength limit [See Eq. (SI-61) in SI-D]. The first two terms of Eq. (39) divided by $2k_{\mathrm{B}}T$ are respectively the same as the two terms of Eq. (1), and so the sum of the two is identical to B for one-component solvents. The last term of Eq. (39) is the contribution from the coupling between the solvent composition and the asymmetric solute-solvent interactions,[36] which is unique to mixture solvents and vanishes at $n_{\mathrm{I}} = 0$ [see Eq. (28)]. The expression in Eq. (39) is formally the same as that of a system composed of a non-ionic binary solvent and a small amount of solute,[36] where the third term can dominate over the other contributions at intermediate solvent compositions. Here (and in SI-A) we have derived Eqs. (38) and (39) in a purely thermodynamic way, while the previous derivation[36] was via the thermodynamic fluctuation theory (see also SI-D).

Our interest is the salt effect on the solute-solute interaction in a dilute electrolyte solvent, and therefore we introduce the salt-enhanced-association (SEA) coefficient,

$$\begin{aligned} C_{\mathrm{I}} &\equiv -\lim_{n_{\mathrm{I}}\to 0}\left(\frac{\partial B}{\partial n_{\mathrm{s}}}\right)_{T,p} \\ &= \frac{-1}{k_{\mathrm{B}}Tn_{\mathrm{w}}}\lim_{n_{\mathrm{I}}\to 0}\left(\frac{\partial U_{\mathrm{hh}}^{\mathrm{eff}}}{\partial X_{\mathrm{I}}}\right)_{T,p}, \end{aligned} \tag{40}$$

where the second equality follows from Eqs. (5), (38) and (SI-13). A positive (resp. negative) value of C_{I} indicates that the salt enhances (resp. reduces) the solute-solute attraction. For later convenience we divide this into two parts $C_{\mathrm{I}} = C_{\mathrm{I}}^{(1)} + C_{\mathrm{I}}^{(2)}$, where $C_{\mathrm{I}}^{(1)}$ is from the first two terms in Eq. (39) and $C_{\mathrm{I}}^{(2)}$ the third term:

$$C_{\mathrm{I}}^{(1)} \equiv \frac{1}{k_{\mathrm{B}}Tn_{\mathrm{w}}}\lim_{n_{\mathrm{I}}\to 0}\left(\frac{\partial[(v_{\mathrm{h}}^{\mathrm{s*}})^2/\kappa_T^{\mathrm{s}} - U_{\mathrm{hh}}^{\mathrm{s}}]}{\partial X_{\mathrm{I}}}\right)_{T,p} \tag{41}$$

$$C_{\mathrm{I}}^{(2)} \equiv \frac{1}{n_{\mathrm{w}}}\lim_{n_{\mathrm{I}}\to 0}(\partial[\chi_{\mathrm{I}}g_{\mathrm{h}}^2]/\partial X_{\mathrm{I}})_{T,p} = K_{\mathrm{S}}^2/4. \tag{42}$$

Here the second equality of Eq. (42) follows from Eqs. (28), (35) and (SI-13). See SI-B for the rather lengthy expression for $C_{\mathrm{I}}^{(1)}$.

Note that in Eq. (42) the numerical factor 4 is specific to 1:1 electrolyte solutions. For a salt with general valence numbers, i.e., $X_aY_b \to aX^{Z_1} + bY^{Z_2}$ with $b = -aZ_1/Z_2$, the numerical factor is replaced by $2(a+b)$. See SI-C for the details.

Partial volumes of individual ion species

The densities can fluctuate about their respective average values even in equilibrium. In particular those of cations and anions can locally be different at times. In long-wavelengths, such density fluctuations can be discussed using the free energy functional $\mathcal{F}[\hat{n}_{\mathrm{w}}, \hat{n}_{\mathrm{c}}, \hat{n}_{\mathrm{a}}, \hat{n}_{\mathrm{h}}]$, where the coarse-grained density variables $\hat{n}_i$ have the Fourier components $\hat{n}_{i\boldsymbol{q}} = \int d\boldsymbol{r}\,\hat{n}_i(\boldsymbol{r})e^{-i\boldsymbol{q}\cdot\boldsymbol{r}}$ with wavenumbers smaller than an upper cut-off $\Lambda < \kappa$. Here the Debye wavenumber is de-

fined as $\kappa = \sqrt{8\pi\ell_B n_{\rm s}}$ with the Bjerrum length $\ell_B = e^2/k_B T \varepsilon$. In the local density approximation, we have the functional of the form[2]

$$\mathcal{F} = \int d\boldsymbol{r} \left[\hat{f}(\hat{n}_{\rm w}, \hat{n}_{\rm c}, \hat{n}_{\rm a}, \hat{n}_{\rm h}) + \frac{\varepsilon(n_{\rm w})|\nabla\Phi|^2}{8\pi} \right]. \tag{43}$$

Here the local free energy $\hat{f}$ includes the fluctuation effects of wavenumbers larger than Λ (e.g., Debye-Hückel (DH) free energy). The second term is the long-range Coulombic interaction, where the electrostatic potential Φ obeys the Poisson equation, $-\nabla \cdot \varepsilon \nabla \Phi = 4\pi e(\hat{n}_{\rm c} - \hat{n}_{\rm a})$.

As is well-known, the density fluctuation variances in the long-wavelength limit are expressed in terms of thermodynamic quantities such as κ_T and $\chi_{\rm I}$ (See SI-D for details). They are closely related to the so-called Kirkwood-Buff integrals (KBIs).[32] The KBIs have been utilized in simulation studies to discuss ion-specificity in electrolyte systems.[22,23,40–43] Shimizu *et al.* have also discussed the ion-specific KBIs using experimental data of water-salt-protein solutions.[44] In the present case, important quantities such as $\chi_{\rm I}$, $K_{\rm S}$, and B can be expressed in terms of KBIs. We shall derive the expressions in SI-E for completeness, while some of them can be found in the literature.[2,23,36,44–46]

The minimum of $\mathcal{F}$ under the constraint of fixed particle numbers gives the thermodynamic Helmholtz free energy, and so we have

$$f(n_{\rm w}, n_{\rm I}, n_{\rm h}) = \hat{f}(n_{\rm w}, n_{\rm I}/2, n_{\rm I}/2, n_{\rm h}). \tag{44}$$

From Eqs. (10) and (44), we readily obtain

$$\kappa_T^{-1} = \sum_{i,j={\rm w,c,a,h}} \hat{f}_{ij} \langle \hat{n}_i \rangle \langle \hat{n}_j \rangle. \tag{45}$$

In analogy with Eqs. (15) and (16), we define the partial volumes of species i $(= {\rm w, c, a, h})$,

$$\bar{v}_i \equiv \kappa_T \sum_{j={\rm w,c,a,h}} \hat{f}_{ij} \langle \hat{n}_j \rangle, \quad \bar{v}_i^* \equiv \bar{v}_i - k_B T \kappa_T. \tag{46}$$

From Eq. (44), this definition is equivalent to Eq. (15) for $i = {\rm w, h}$, and the following relations follow for $i = {\rm c, a}$:

$$\bar{v}_{\rm c} + \bar{v}_{\rm a} = 2\bar{v}_{\rm I}, \quad \bar{v}_{\rm c}^* + \bar{v}_{\rm a}^* = 2\bar{v}_{\rm I}^*. \tag{47}$$

As in the same manner as in Eqs. (18) and (19), we also define the symbols $v_i^{\rm s}$, $v_i^{\rm s*}$, v_i, and v_i^* for $i = {\rm c, a}$ as the ion partial volumes in the limiting cases, $n_{\rm h} \to 0$, and $n_{\rm h}, n_{\rm I} \to 0$.

The salt partial volumes $2\bar{v}_{\rm I}$ of many salts have been measured in experiments,[47,48] and many authors have attempted to separate experimental salt partial volumes for infinitely dilute electrolyte solutions into cation and anion contributions, i.e., $v_{\rm c}$ and $v_{\rm a}$, by assigning, for example, the partial volume of H^+ a value of zero, and by assuming additive, independent contribution from each ion species.[47] The latter assumption is valid for infinitely dilute electrolyte solutions in which the contribution from the ion-ion interactions is negligible. While it seems difficult to thermodynamically determine $v_{\rm c}$ and $v_{\rm a}$ since the cation and anion numbers cannot be changed independently, Zana and Yeager (1967) have measured dynamical responses (ionic vibration potential) of electrolyte solutions to ultrasonic waves to determine individual ionic volumes without assuming any value of any ionic volume.[47,49]

Model local free energy

We introduce a model for the local free energy density $\hat{f}(\hat{n}_{\rm w}, \hat{n}_{\rm c}, \hat{n}_{\rm a}, \hat{n}_{\rm h})$. Once this is done, all the thermodynamic quantities discussed in the previous section can be calculated since the Helmholtz free energy density f is given by Eq. (44) in terms of $\hat{f}$. Specifically, we shall numerically investigate $K_{\rm S}$ and $C_{\rm I}$ defined respectively in Eqs. (31) and (40), varying the ion and solute sizes.

In our model, the steric and hydration (electrostriction) effects shall be taken into account, using the Boublík-Mansoori-Carnahan-Starling-Leland (BMCSL) model for hard-sphere mixtures[37,38] and the Born model,[39] respectively. This is a straightforward generalization of the previous model[2] for aqueous electrolyte solutions, which can semi-quantitatively explain the puzzling behavior

of the ion-specificity in the salt activity coefficient, osmotic coefficient, and salt partial volume.

We assume that the model local free energy density $\hat{f}$ consists of five parts,

$$\hat{f} = k_B T \sum_{i=\text{w,c,a,h}} \hat{n}_i [\ln(\hat{n}_i \lambda_i^3) - 1] \\ + \hat{f}_\text{h} + \hat{f}_\text{a} + \hat{f}_\text{B} + \hat{f}_\text{DH}. \quad (48)$$

The first term is the entropic contribution of an ideal mixture, where λ_i is the thermal de Broglie length of species i. The second term $\hat{f}_\text{h}$ is the free energy of the steric interactions; we use BMCSL model for four-component hard-sphere mixtures,[37,38] where each species has a hard-sphere diameter d_i ($i = $ w, c, a, h). The third term $\hat{f}_\text{a}$ arises from the short-range attraction (van der Waals force). For moderately varying densities, $\hat{f}_a$ is given by the van der Waals form, $\hat{f}_\text{a} = -\frac{1}{2} \sum_{i,j=\text{w,c,a,h}} w_{ij} \hat{n}_i \hat{n}_j$. The interaction coefficient w_{ij} is determined from the integration of the attractive part of the Lennard-Jones (LJ) potential,[2,36,50–52] $w_{ij} = (32\sqrt{2}/9)\pi \epsilon_{ij} d_{ij}^3$, where ϵ_{ij} and d_{ij} are the LJ energy and size parameters, respectively. We set the size parameter using the hard-sphere diameter as $d_{ij} = (d_i + d_j)/2$. The hydrogen bond, which does *not* stem from the LJ interactions, causes many unique behaviors of water.[53,54] In our model, however, we effectively include the water-water attraction due to hydrogen bond into $\hat{f}_\text{a}$ by tuning the parameter ϵ_ww.

For ion-hydration free energy we use the simple Born model,[39] $\hat{f}_\text{B} = k_B T \sum_{i=\text{c,a}} \hat{n}_i [\ell_B(\hat{n}_\text{w}) - \ell_B(0)]/2R_i$, where $R_i (\sim d_i/2)$ is the Born radius. Here we assume the Bjerrum length $\ell_B = e^2/k_B T \varepsilon(\hat{n}_\text{w})$ depends only on the solvent density $\hat{n}_\text{w}$, but not explicitly on the solute density $\hat{n}_\text{h}$. To the best of authors' knowledge, there are no experimental data of ε for aqueous solutions of nonpolar solutes. However, this assumption can be justified as follows. The polarization density p_e of the solution is a function of n_w only, under the assumptions that the nonpolar solute has no dipole moment and that the solute does not affect the dipole moment of water molecules; the dielectric permittivity ε is determined by the polarization density p_e

using, for example, the Kirkwood's expression $p_\text{e} = (\varepsilon - 1)(2\varepsilon + 1)/9\varepsilon$. In theories for dielectric permittivity of polar mixture fluids, similar assumptions have been made that the dipole moment of each component is not affected by mixing.[55,56]

Note, even though ε has no explicit dependence on the solute density n_h, ε depends on n_h in *isobaric* condition because a change in n_h is accompanied by that in the water density n_w. To be more explicit, we have $\lim_{n_\text{h} \to 0}(\partial \varepsilon/\partial n_\text{h})_p = -(\partial \varepsilon/\partial p)v_\text{h}/\kappa_\text{w}$, where in the right hand side the derivative is taken for pure water at $n_\text{h} = 0$ (see also SI-F).

One may claim that the Born energy is not a "short-ranged" one, as it is an integration of the electrostatic energy over the whole space around an isolated charged sphere of radius R_i. However, the electrostatic energy is concentrated in the vicinity of the ion, so that we may regard this as a short-range interaction between ions and the solvent molecules. For an ion with a Born radius 1Å, the electrostatic energy within the third hydration radius ($\sim$ 10Å) is about 90% out of the total Born energy.

The last term $\hat{f}_\text{DH}$ in Eq. (48) is the Debye-Hückel free energy,[57] which stems from the charge fluctuations on the length-scale shorter than the Debye length κ^{-1}. It is given by $\hat{f}_\text{DH} = -k_B T \hat{\kappa}^3/12\pi + (1/2)\sum_{i,j=\text{c,a}} u_{ij}^\text{ex} \hat{n}_i \hat{n}_j + \cdots$ to second order in $\hat{n}_\text{c}$ and $\hat{n}_\text{a}$, where $\hat{\kappa}(\hat{n}_\text{w}, \hat{n}_\text{c}, \hat{n}_\text{a})$ is the fluctuating Debye wavenumber[2] defined in Eq. (SI-43), and the coefficient u_{ij}^ex may depend both on $\hat{n}_\text{w}$ and $\hat{n}_\text{h}$. It turns out that $\hat{f}_\text{DH}$ is not relevant to K_S and C_I that we shall examine numerically. This can be understood as follows. The coefficients K_S and C_I include the derivatives of $\hat{f}_\text{DH}$ with respect to $\hat{n}_i$ ($i = $ w, c, a, h) in the limit $\hat{n}_\text{c} = \hat{n}_\text{a} = n_\text{s} \to 0$. However, we can confirm that the orders of $\hat{n}_\text{c}$- and $\hat{n}_\text{a}$-derivatives are at most one, so that all these terms vanish in the limit $n_\text{s} \to 0$.

Selected parameter values

The parameter values for the solvent (water) and ions are the same as those in the previous paper.[2] We do not study temperature dependence, so that it is kept fixed at $T = $

300 K. For the solvent, we set $d_{\mathrm{w}} = 3\,\text{Å}$ and $\epsilon_{\mathrm{ww}} = 412.72\,\text{K}$. These values are chosen so that the isothermal compressibility at $p = 1\,\text{atm}$ and $T = 300\,\text{K}$ coincides with the experimental value of water, $\kappa_{\mathrm{w}} = 4.5 \times 10^{-4}\,\text{MPa}^{-1}$. On the other hand, this choice slightly underestimates the density of pure water, $n_{\mathrm{w}0} = 0.857/d_{\mathrm{w}}^3 \approx 31.7\,\text{nm}^{-3}$. For the ions and solute, the LJ parameters ϵ_{ii} between the same particle species are set all equal to 200 K: $\epsilon_{\mathrm{cc}} = \epsilon_{\mathrm{aa}} = \epsilon_{\mathrm{hh}} = 200\,\text{K}$. We assume the Lorentz-Berthelot relation $\epsilon_{ij} = \sqrt{\epsilon_{ii}\epsilon_{jj}}$ for $i \neq j$; we then have $\epsilon_{\mathrm{ca}} = \epsilon_{\mathrm{ch}} = \epsilon_{\mathrm{ah}} = 200\,\text{K}$ and $\epsilon_{\mathrm{wc}} = \epsilon_{\mathrm{wa}} = \epsilon_{\mathrm{wh}} = 287.30\,\text{K}$. In reality, the ϵ_{ij}-values should differ for different ions and solutes, and hence one can vary the ϵ_{ij}-values simultaneously with the changes of ion- and solute-diameters, which may give a better fit to the experimental data. However, changes of these parameter-values within a reasonable range do not alter the general trend of ion- and solute-size dependencies of the thermodynamic quantities, and hence we keep them fixed not to complicate the study.

In the following numerical analysis, the ion hard-sphere diameter d_i $(i = \mathrm{c}, \mathrm{a})$ and Born radius R_i $(i = \mathrm{c}, \mathrm{a})$ are varied, whereas the ratio R_i/d_i is kept fixed at $R_i/d_i = 0.2$ $(i = \mathrm{c}, \mathrm{a})$. The Born model with this parameter choice combined with the BMCSL model gives a good estimation of ion partial volumes,[2] while the Born model is a crude one for ion hydration.

The value of the dielectric permittivity ε at $p = 1\,\text{atm}$ and $T = 300\,\text{K}$ is selected so that the Bjerrum length coincides with that of water, $\ell_B(n_{\mathrm{w}}) = 7\,\text{Å}$. Measurements of the water dielectric constant under various pressure[58,59] give $\varepsilon^{-1}(\partial\varepsilon/\partial p)_T \approx 5 \times 10^{-4}\,\text{MPa}^{-1}$, and hence we set $a_\varepsilon \equiv n_{\mathrm{w}}\varepsilon^{-1}(\partial\varepsilon/\partial n_{\mathrm{w}}) = \varepsilon^{-1}(\partial\varepsilon/\partial p)_T/\kappa_{\mathrm{w}} = 1.1$. Finally, to calculate C_{I}, we set $A_{\mathrm{B}} \equiv (\partial^2\varepsilon/\partial p^2)/(\varepsilon\kappa_{\mathrm{w}}^2 a_\varepsilon) - 2a_\varepsilon = -7.5$.

We make some remarks. (i) With our model, the high-order derivatives of the free energy can somewhat deviate from those of water. Specifically, our model gives $n_{\mathrm{w}}(\partial\kappa_{\mathrm{w}}/\partial n_{\mathrm{w}})/\kappa_{\mathrm{w}} \approx -5.4$, which deviates from the experimental value -8.33 of water.[60] We have correspondingly set[2] $A_{\mathrm{B}} = -7.5$, while the experimental data of water dielectric permittivity gives[58,59]

$\varepsilon^{-1}\partial^2\varepsilon/\partial p^2 \approx -6 \times 10^{-7}\,\text{MPa}^{-2}$ which yields $A_{\mathrm{B}} \approx -5$. (ii) In general, cations and anions interact differently with solvent molecules; in water, cations tend to attract hydrogen atoms of water, while anions favor an oxygen atoms.[61] For simplicity, however, we do not differentiate the properties of (monovalent) cations and anions except the signs of the charges and the diameters d_i $(i = \mathrm{c}, \mathrm{a})$. Hence all the numerical results in the following are invariant under the exchange of d_{c} and d_{a}.

Results and Discussion

For the sake of lighter notation we introduce the normalized hard-sphere diameters of the ions and solute

$$\alpha_i \equiv d_i/d_{\mathrm{w}} \quad (i = \mathrm{c}, \mathrm{a}, \mathrm{h}). \tag{49}$$

In the following we shall numerically examine the Sechenov coefficient K_{S} and the SEA coefficient C_{I} defined in Eq. (40), varying α_{c}, α_{a}, and α_{h}.

Sechenov coefficient

Figures 1a and 1c present the calculated normalized Sechenov coefficient $K_{\mathrm{S}}/d_{\mathrm{w}}^3$ as a function of the cation diameter α_{c} for the fixed anion diameters $\alpha_{\mathrm{a}} = 0.7$ and 1.3, respectively. In each panel the solute diameter α_{h} is set equal to 1.4, 1.2, 1.0, 0.8, and 0.6. In Figures 1b and 1d surface plots are also shown as a function of α_{c} and α_{h} for $\alpha_{\mathrm{a}} = 0.7$ and 1.3, respectively. Note that the exchange of α_{c}- and α_{a}-values gives exactly the same result. We observe that (i) K_{S} decreases as the ion-size increases, (ii) K_{S} increases as the solute size α_{h} increases for not very large ions (in the whole plot-range of Figures 1a and 1b, and $\alpha_{\mathrm{c}} \lesssim 0.9$ in 1c and 1d), (iii) for large ions ($\alpha_{\mathrm{c}} \gtrsim 0.9$ in Figures 1c and 1d), the α_{h}-dependence of K_{S} is inverted, so that K_{S} decreases as α_{h} increases, and (iv) K_{S} can be negative for large ions and solutes as shown in Figures 1c and 1d.

In Table 1 experimental data of Sechenov coefficient K_{S} are listed for hydrogen, oxygen, and benzene in alkali metal halide solutions. The
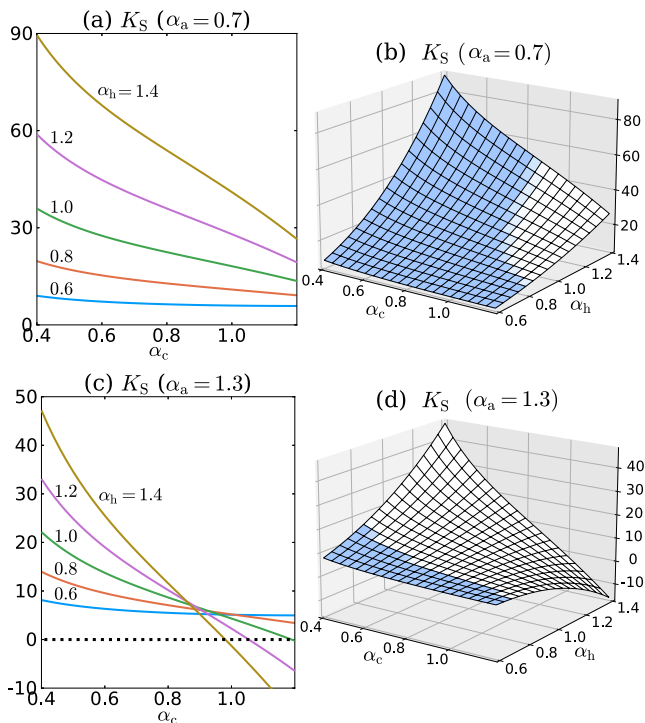
Figure 1: Normalized Sechenov coefficient K_S/d_w^3 vs cation diameter $\alpha_c = d_c/d_w$ for (a) $\alpha_a = d_a/d_w = 0.7$ and (c) 1.3. In each panel we set the normalized solute diameter $\alpha_h = d_h/d_w$ to 1.4, 1.2, 1.0, 0.8, and 0.6. Surface plots of K_S/d_w^3 as a function of α_c and α_h are also presented for (b)$\alpha_a = 0.7$ and (d)1.3. In (b) and (d) the pale-blue color indicates the region where $K_S \approx K_S^{el}$ is a good approximation.

general trend of the data is fairly consistent with the above four features of our theoretical curves, whereas one exception is the values for Li$^+$ that is the smallest cation in size. We shall later discuss this rather irregular behavior of Li$^+$.

To study K_S in detail, we divide the (standard) ion partial volume v_i ($i = $ c, a) into two parts,

$$v_i = v_i^{int} + v_i^{el}, \quad (i = c, a) \qquad (50)$$

where "intrinsic" volume v_i^{int} is the partial volume without the electrostriction effect[48,62,63] and is comparable to the molecular size. The second term v_i^{el} (< 0) is the electrostriction volume, which arises from the polarization of the solvent molecules (electric dipoles) around the ion. Using Eq. (50), we can also divide the Sechenov coefficient K_S in Eq. (31) into two parts, $K_S = K_S^{int} + K_S^{el}$; K_S^{int} is due to the steric effect and the short-range attractive interactions (i.e., $\hat{f}_h$ and f_a in our model) when the electrostriction is "turned off," and K_S^{el} is the additional contribution when the electrostriction is "turned on." Since we assume the solute is non-polar, we may generally neglect the electrostriction effect on U_{hI}; in fact, the Born model $\hat{f}_B$ that we use in the numerical analysis is irrelevant to U_{hI} since we assume the dielectric permittivity ε does not depend on the solute density n_h at fixed n_w (note, however, ε varies as n_h is changed in *isobaric* condition for which an increase in n_h induces a decrease in n_w). The solute partial volume v_h^* is also free from the electrostriction effect, so that we have

$$k_B T K_S^{int}/2 = U_{hI} - v_h^* v_I^{int}/\kappa_w \qquad (51)$$

$$k_B T K_S^{el}/2 = -v_h^* v_I^{el}/\kappa_w, \qquad (52)$$

where $v_I^{int} = (v_c^{int} + v_a^{int})/2$ and $v_I^{el} = (v_c^{el} + v_a^{el})/2$.

The combination of the BMCSL model $\hat{f}_h$ and the attraction contribution $\hat{f}_a$ gives[2] $v_i^{int} \sim \alpha_i^3$ for not too small α_i. With our model the electrostriction volume v_i^{el} is the Drude-Nernst

10

Table 1: Sechenov coefficient K_S in units of L/mol ($\approx 62d_w^3$) for non-polar gases in alkali metal halide solutions. (a) Long and McDevit[15] (b) Hermann et al.[18]

	LiCl	NaCl	KCl	RbCl	CsCl	CsI
hydrogen	0.17[a]	0.26[a]	0.23[a]	0.21[b]	0.18[b]	0.15[b]
oxygen	0.23[a]	0.32[a]	0.30[a]	0.25[b]	0.22[b]	0.19[b]
benzene	0.32[a]	0.46[a]	0.39[a]	0.32[a]	0.21[a]	-0.014[a]

form[2,64] derived from Born energy $\hat{f}_B$,

$$v_i^{el} = v_i^B \equiv \frac{k_B T n_w \kappa_w}{2R_i} \frac{\partial \ell_B}{\partial n_w} = -k_B T \kappa_w \ell_B a_\varepsilon / 2R_i, \tag{53}$$

where a_ε has been defined in the section of Selected parameter values. It turns out in SI-F that K_S^{el} in Eq. (52) with the Drude-Nernst electrostriction volume in Eq. (53) can also be derived from Debye-McAulay theory.[15,26] Our parameter choice gives[2]

$$v_i^{int} \approx D_L d_w^3 \alpha_i^3, \quad v_i^B = -D_B d_w^3 / \alpha_i \tag{54}$$

with $D_L \approx 1.1$ and $D_B = 0.44$.

The plotted in Figures 2a and 2c are K_S^{int} as a function of α_c for the fixed anion diameters $\alpha_a = 0.7$, and 1.3, respectively. Except for negligibly small positive values at $\alpha_h = 0.6$, K_S^{int} is negative and decreases as α_c and α_h increase. Using Eqs. (14) and (44), we can rewrite Eq. (51) as $k_B T K_S^{int} = \sum_{i=c,a}[U_{hi} - v_h^* v_i^{int}/\kappa_w]$, where $U_{hi} = \lim_{n_I,n_h \to 0} \hat{f}_{hi}$. As discussed previously,[2] effective interactions without electrostriction is mostly negative (attractive) and is roughly approximated as $[U_{hi} - v_h^* v_i^{int}/\kappa_w]/k_B T d_w^3 \sim -(\alpha_h^3 + \alpha_i^3)^2$. This approximation becomes accurate as α_h and/or α_i become large. Within this approximation we have

$$K_S^{int}/d_w^3 \sim -\sum_{i=c,a}(\alpha_h^3 + \alpha_i^3)^2. \tag{55}$$

Let us evaluate the right hand side (RHS) of Eq. (55) in some cases. (i) At $\alpha_c = 0.4$ (the lower bound of the horizontal axis) in Figure 2a, RHS of Eq. (55) is equal to -2.9, -7.5, and -17.4 for $\alpha_h = 1.0$, 1.2, and 1.4, respectively. (ii) At $\alpha_c = 1.2$ (the upper bound of the horizontal axis) in the same panel, it is -9.2, -16.2, and -29.5 for $\alpha_h = 1.0$, 1.2, and 1.4, respectively.
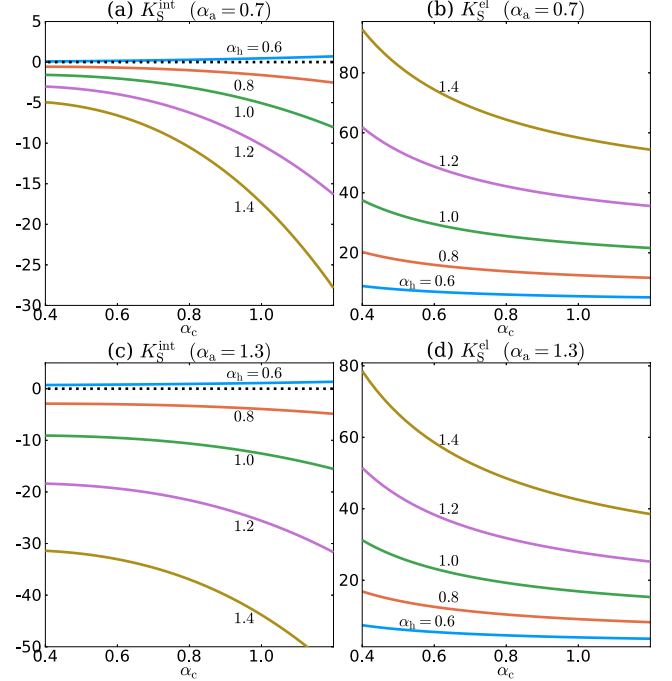

Figure 2: The normalized pseudo-Sechenov coefficient K_S^{int}/d_w^3 *without Born energy* vs cation diameter $\alpha_c = d_c/d_w$ for (a) $\alpha_a = d_a/d_w = 0.7$ and (c) 1.3. The difference between the full Sechenov coefficient K_S and K_S^{int}, i.e., $K_S^{el} = K_S - K_S^{int}$ for (b) $\alpha_a = 0.7$ and (d) 1.3. In each panel the normalized solute diameter $\alpha_h = d_h/d_w$ is set to 1.4, 1.2, 1.0, 0.8, and 0.6.

(iii) At $\alpha_c = 0.4$ in Figure 2b, it is -11.4, -18.6, and -32.3 for $\alpha_h = 1.0$, 1.2, and 1.4, respectively. (iv) At $\alpha_c = 1.2$ in the same panel, it is -17.7, -27.3, and -44.4 for $\alpha_h = 1.0$, 1.2, and 1.4, respectively. While in the case (i) the RHS of Eq. (55) overestimates the value of K_S^{int}, it captures the overall behavior of K_S^{int} as we can see from the other examples (ii)–(iv).

Regarding K_S^{el}, as in the case of v_i^{int} the com-

bination of $\hat{f}_\mathrm{h}$ and $\hat{f}_\mathrm{a}$ gives $v_\mathrm{h}^* \approx d_\mathrm{w}^3 \alpha_\mathrm{h}^3$, so that

$$K_\mathrm{S}^\mathrm{el}/d_\mathrm{w}^3 \approx H\alpha_\mathrm{h}^3(\alpha_\mathrm{c}^{-1} + \alpha_\mathrm{a}^{-1}), \qquad (56)$$

where $H = D_\mathrm{B} d_\mathrm{w}^3/k_\mathrm{B}T\kappa_\mathrm{w} = 6.4$. In Figures 2b and 2d K_S^el is plotted as a function of α_c for $\alpha_\mathrm{a} = 0.7$ and 1.3, respectively. We can see that K_S^el decreases as the ion sizes α_c and α_a increase, whereas it increases as the solute size increases. The approximate expression (56) explains these features.

We now discuss the overall behavior of K_S in Figures 1a–1d, using Eqs. (55) and (56). (i) If the cation is smaller than the solute in size ($\alpha_\mathrm{c} < \alpha_\mathrm{h}$) we can neglect α_c-dependence of $K_\mathrm{S}^\mathrm{int}$ to have $K_\mathrm{S}/d_\mathrm{w}^3 \sim K_\mathrm{S}^\mathrm{el}/d_\mathrm{w}^3 - \alpha_\mathrm{h}^6 - (\alpha_\mathrm{h}^3 + \alpha_\mathrm{a}^3)^2$; the α_c-dependence of K_S for small α_c in Figures 1a and 1c solely comes from $K_\mathrm{S}^\mathrm{el}/d_\mathrm{w}^3$. (ii) Furthermore, when α_c is small such that $\alpha_\mathrm{c} \ll H/\alpha_\mathrm{h}^3, H/\alpha_\mathrm{a}^3$, we can neglect $K_\mathrm{S}^\mathrm{int}$ and hence have $K_\mathrm{S} \approx K_\mathrm{S}^\mathrm{el}$. This means Debye-McAulay theory becomes more plausible for small ions and solutes. In Figures 1b and 1c the pale-blue color indicates the region where $0.9 < K_\mathrm{S}^\mathrm{el}/K_\mathrm{S} \lesssim 1.25$. (iii) Because K_S^el is always positive, the negative K_S value for large ions and solutes in Figure 1c is due to $K_\mathrm{S}^\mathrm{int}$, i.e., the combination of steric effects and short-range attraction. (iv) To discuss the inversion of α_h-dependence of K_S in Figures 1c and 1d, we consider the inequality $\partial K_\mathrm{S}/\partial(\alpha_\mathrm{h}^3) > 0$, which yields

$$H\alpha_\mathrm{c}^{-1} - 2\alpha_\mathrm{c}^3 > 4\alpha_\mathrm{h}^3 - H\alpha_\mathrm{a}^{-1} + 2\alpha_\mathrm{a}^3 \qquad (57)$$

within the approximations of Eqs. (55) and (56). Here the left hand side (LHS) is a monotonic decreasing function of α_c that varies from ∞ to $-\infty$ in the range $0 < \alpha_\mathrm{c} < \infty$, so that the inequality holds when α_c is smaller than a threshold value $\alpha_\mathrm{c,th}$ determined by α_a and α_h; α_h-dependence is reversed at $\alpha_\mathrm{c} = \alpha_\mathrm{c,th}$. We also notice that the RHS of Eq. (57) is an increasing function of α_a, and hence the threshold value $\alpha_\mathrm{c,th}$ decreases as α_a increases. Equating the LHS to RHS of Eq. (57), we obtain, for example, $\alpha_\mathrm{c,th} = 1.44$ at $(\alpha_\mathrm{a}, \alpha_\mathrm{h}) = (0.7, 1.2)$, and 0.84 at (1.3, 1.2); this explains the reason why we can see the inversion of α_h-dependence in

Figure 1c but not in the plot-range of 1a.

We make remarks on the irregular behavior of K_S for Li$^+$. In Table 1, the values of K_S for LiCl is smaller than the corresponding values of NaCl. This contradicts our theoretical result and the general trend of the experimental data that ions with smaller sizes tend to have larger values of K_S. This irregular behavior of Li$^+$ has been reproduced in all-atom MD simulations,[22,23] but cannot be captured by our simple model. While microscopic (molecular level) modeling seems necessary for a full understanding,[23] we can partly understand this behavior using the divisions in Eqs. (50) and (52). We may make these divisions without assuming Born model for the electrostriction effect. Since Li$^+$ is small in size, we neglect $K_\mathrm{S}^\mathrm{int}$ and have $K_\mathrm{S} \approx K_\mathrm{S}^\mathrm{el} = -v_\mathrm{h}^* v_\mathrm{I}^\mathrm{el}/\kappa_\mathrm{w}$. Meanwhile, attempts have been made to evaluate electrostriction volumes v_I^el from experimental salt partial volumes of various salts, under some assumption for the intrinsic volume $v_\mathrm{I}^\mathrm{int}$; there have been some variations, but all assume $v_\mathrm{I}^\mathrm{int}$ to be comparable to the molecular volumes.[63] With a reasonable choice of $v_\mathrm{I}^\mathrm{int}$, the evaluated electrostriction volumes are -13.0 and -7.2 in units of cm^3/mol for NaCl and LiCl, respectively.[48] That is, the electrostriction effect on the ion partial volume is weaker for LiCl than for NaCl, which opposes the result of Born model in Eq. (53) that predicts smaller ions give stronger electrostriction effect. This irregular electrostriction volume of Li$^+$ is the source of the smaller value of $K_\mathrm{S} \approx -v_\mathrm{h}^* v_\mathrm{I}^\mathrm{el}/\kappa_\mathrm{w}$ for LiCl than for NaCl. Recently, the correlation between K_S and v_I has also been discussed using MD simulations of methane-salt-water solutions.[23]

Salt-enhanced-association (SEA) coefficient

We now examine the SEA coefficient C_I defined in Eq. (40). In Figures 3a and 3b the normalized SEA coefficient $C_\mathrm{I}/d_\mathrm{w}^6$ is plotted as a function of the cation diameter α_c for the fixed anion diameters $\alpha_\mathrm{a} = 0.7$ and 1.3, respectively. In each panel the solute diameter α_h is set to 1.4, 1.2, 1.0, 0.8, and 0.6. In Figures 4a and 4b surface plots of C_I in the $(\alpha_\mathrm{c}, \alpha_\mathrm{h})$-plane are

also presented for $\alpha_\mathrm{a} = 0.7$ and 1.3, respectively. They show that C_I is positive in most of the plot ranges, which means that an addition of ions usually shifts the solute-solute interaction towards attraction. We also notice that the ion effect is stronger for larger solutes and for smaller ions.

In Figures 3a and 3b the plotted in broken lines are the contribution $C_\mathrm{I}^{(2)} = K_\mathrm{S}^2/4$ from the coupling between the solvent composition and the asymmetric solute-solvent interactions (see Eq. (42)). We notice that the curves of $C_\mathrm{I}^{(2)}$ behave similarly to those of C_I. Figures 3c and 3d present the plots of C_I vs $C_\mathrm{I}^{(2)}$, where the parameters are the same as in Figures 3a and 3b, respectively. In the entire plot-range, we observe that

$$C_\mathrm{I} \approx C_\mathrm{I}^{(2)} = K_\mathrm{S}^2/4. \tag{58}$$

Figures 3e and 3f show the plots of C_I vs K_S with marks and $C_\mathrm{I}^{(1)}$ vs K_S with dashed lines. These also confirm the validity of the approximate relation Eq. (58); $C_\mathrm{I}^{(1)}$ also varies with K_S, but the correlation is much weaker than that between the total SEA coefficient C_I and K_S.

Equation (58) approximately quantifies the correlation between the two different salt effects: the one on the solubility of solutes and the other on the solute-solute effective interaction. Because a change in solvent-solvent and solute-solvent molecular interactions crucially influences both the solubility and effective interaction, it is not surprising K_S and C_I are somehow correlated. However, how they are correlated is by no means trivial, as the former is determined for a single, isolated solute molecule in the solvent. In principle, the osmotic second virial coefficients B is extracted from, for instance, the n_h-dependence of solute activity. However, such experiments would be very difficult when the solubility of a solute is extremely low as in the present case, and to the best of the authors' knowledge, no experimental data of B for nonpolar solutes in water with nor without salt are available in the literature. Hence at present computer simulation is the only effective tool to check our theoretical
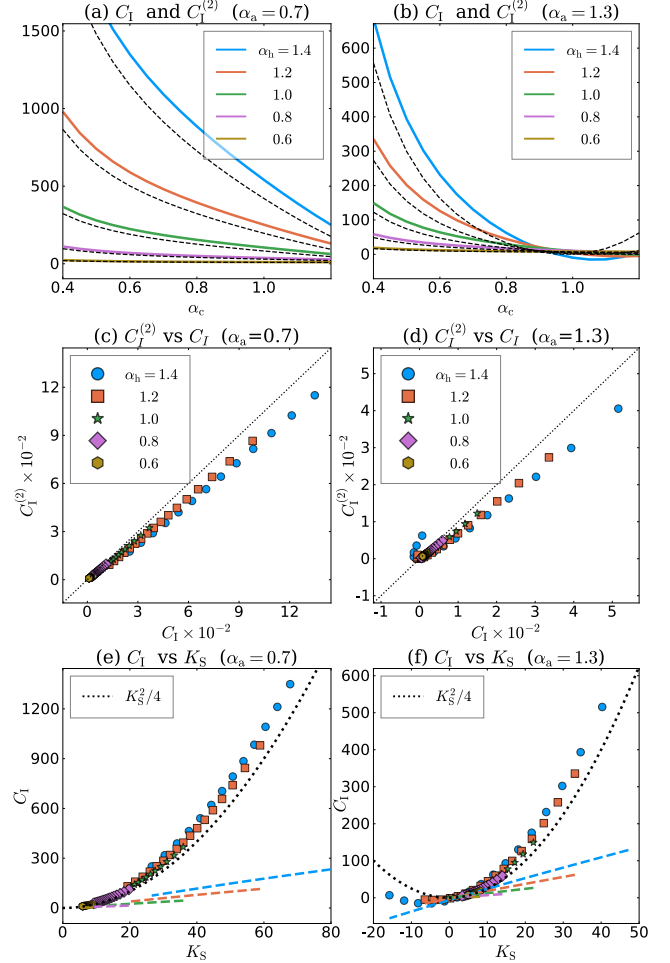

Figure 3: (a) and (b): The normalized SEA coefficients $C_\mathrm{I}/d_\mathrm{w}^6$ (solid lines) and $C_\mathrm{I}^{(2)}/d_\mathrm{w}^6$ (broken lines) as functions of the cation diameter $\alpha_\mathrm{c} = d_\mathrm{c}/d_\mathrm{w}$. (c) and (d): C_I vs $C_\mathrm{I}^{(2)}$ in units of $d_\mathrm{w}^6 10^2$. (e) and (f): $C_\mathrm{I}/d_\mathrm{w}^6$ vs $K_\mathrm{S}/d_\mathrm{w}^3$. Each mark-shape corresponds to its respective α_h-value shown in (c) and (d). The dashed lines present $C_\mathrm{I}^{(1)}/d_\mathrm{w}^6$, where each line color corresponds to the α_h-value of the mark with the same color. The normalized anion diameter $\alpha_\mathrm{a} = d_\mathrm{a}/d_\mathrm{w}$ is set to 0.7 in (a), (c), and (e), and to 1.3 in (b), (d), and (f). In each panel the normalized solute diameter $\alpha_\mathrm{h} = d_\mathrm{h}/d_\mathrm{w}$ is set to 1.4, 1.2, 1.0, 0.8, and 0.6.

(a) C_I ($\alpha_a = 0.7$)
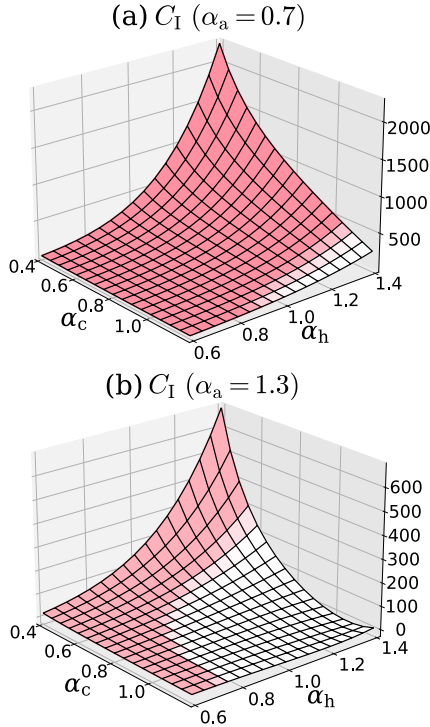
(b) C_I ($\alpha_a = 1.3$)

Figure 4: Surface plots of the normalized SEA coefficient C_I/d_w^6 as a function of the cation diameter $\alpha_c = d_c/d_w$ and the solute diameter $\alpha_h = d_h/d_w$ for (a) $\alpha_a = d_a/d_w = 0.7$ and (b)1.3. The pale-red color indicates the region of $|C_I^{(1)}/C_I^{(2)}| \lesssim 1/3$.

prediction.

Thomas and Elcock[31] performed MD simulations to investigate how additions of alkali-halide salts affect the solute-solute PMFs of methane and neopentane solutions. They found that the salts with larger K_S-values tend to lower the PMFs more abundantly in a wide range of the solute-solute distance, which suggests their simulation data is at least qualitatively consistent with Eq. (58).

More recently, Koga and Yamamoto[33] have studied the correlation between the excess solute chemical potential $k_B T \nu_h^s$ and the second osmotic virial coefficient B of methane in a NaCl-water solution, using MD simulations. From their simulation data, we estimate $B \approx -0.02\,\mathrm{L/mol}$ without salt and $B \approx -0.10\,\mathrm{L/mol}$ at $n_s \approx 1\,\mathrm{mol/L}$, which yields $C_I \approx 0.08\,\mathrm{L^2/mol^2}$. Here we have used Eq. (SI-67) to obtain the solute-solute KBI $G_{hh}^s = -2B$ in the limit $n_h \to 0$ from the KBI G_{hh} computed at $n_h \approx 0.67\,\mathrm{mol/L}$, while Koga and Yamamoto[33] have simply approximated as $B \approx -G_{hh}/2 \approx -0.12$. We also estimate $K_S \approx 0.51\,\mathrm{L/mol}$ from the data of $k_B T \nu_h^s$ in Koga and Yamamoto, which yields $C_I^{(2)} \approx 0.065\,\mathrm{L^2/mol^2}$. We hence have $C_I^{(2)}/C_I \approx 0.81$, and Eq. (58) holds fairly well.

Note, meanwhile, that Eq. (58) does not always mean $|C_I^{(1)}/C_I^{(2)}| \ll 1$. The plotted in Figures 5a and 5b are the ratio $C_I^{(2)}/C_I$ as a function of α_c (Note that α_c in Figure 5b is restricted in the range such that $C_I < 0$, while in Figure 3b C_I becomes positive from negative at around $\alpha_c \approx 0.9$.). The pale-red color in Figures 4a and 4b indicates the region where $|C_I^{(1)}/C_I^{(2)}| \lesssim 1/3$. They show the tendency that $|C_I^{(1)}/C_I^{(2)}| \ll 1$ (or $C_I^{(2)}/C_I \sim 1$) is violated for large ions and/or solutes, for which both K_S and $|C_I|$ are small.

In summary, the approximation in Eq. (58) is good in a sense that $|C_I^{(1)}/C_I^{(2)}| \ll 1$, when the ions and/or solutes are small in size, $\alpha_c, \alpha_a, \alpha_h \lesssim 1$. Otherwise the inequality $|C_I^{(1)}/C_I^{(2)}| \ll 1$ is violated; even in this case, as is shown in Figures 3c–3f we can nevertheless use Eq. (58) for a rough estimate of the SEA coefficient C_I from the Sechenov coefficient K_S.

14
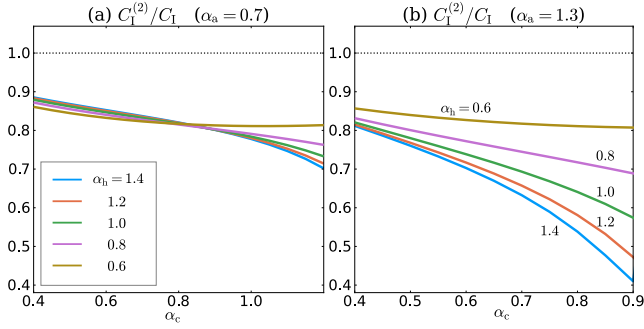
Figure 5: $C_{\mathrm{I}}^{(2)}/C_{\mathrm{I}}$ vs α_{c}. The normalized anion diameter $\alpha_{\mathrm{a}} = d_{\mathrm{a}}/d_{\mathrm{w}}$ is set to 0.7 in (a), and to 1.3 in (b). In each panel the normalized solute diameter $\alpha_{\mathrm{h}} = d_{\mathrm{h}}/d_{\mathrm{w}}$ is set to 1.4, 1.2, 1.0, 0.8, and 0.6.

Conclusions

We have investigated the salt effects on the gas solubility (the solute excess chemical potential $k_{\mathrm{B}}T\nu_{\mathrm{h}}^{\mathrm{s}}$) and the effective solute-solute interaction (second osmotic virial coefficient B or the effective interaction coefficient $U_{\mathrm{hh}}^{\mathrm{eff}}$). The former is measured by the Sechenov coefficient K_{S} and the latter by the SEA (salt-enhanced-association) coefficient C_{I} defined in Eqs. (31) and (40), respectively. In our study the densities of water, ions, and solutes are explicitly regarded as the variables, so that solvent-mediated interactions are naturally taken into account.[2,36]

We have first introduced some basic thermodynamic quantities such as the solute excess chemical potential $\nu_{\mathrm{h}}^{\mathrm{s}}$, the partial volumes $\bar{v}_i$, v_i^{s} and v_i, and the solvent composition susceptibility χ_{I}. Then in terms of these quantities we have expressed the Sechenov coefficient K_{S} and the effective interaction coefficient $U_{\mathrm{hh}}^{\mathrm{eff}}$; the expressions in Eqs. (31)–(33), and (39) are generalization of Eq. (1). In Eq. (39) the term $-k_{\mathrm{B}}T\chi_{\mathrm{I}}g_{\mathrm{h}}^2$, where g_{h} measures the asymmetry between the solute-salt and solute-water interactions, is due to the coupling of composition susceptibility and the asymmetric solute-solvent interactions. Previously,[36] the same expression has been derived for the solute-solute effective interaction coefficient in a non-ionic ternary mixture composed of a solute and a bi-

nary solvent, using thermodynamic fluctuation theory; the previous result can be used by regarding the cations and anions as a single indistinguishable component. To quantify the salt effect on the solute-solute effective interaction, the SEA coefficient C_{I} has been introduced as the coefficient of the second-order term of the expansion of the second osmotic virial coefficient B in powers of the salt density in Eq. (40). We have also introduced, in terms of the coarse-grained local free energy density $\hat{f}$, the partial volumes of individual ion species, which play important roles in understanding the ion-size dependence of K_{S}.

We have modeled the local free energy density using the four-component (water, cation, anion, and solute) BMCSL (Boublík-Mansoori-Carnahan-Starling-Leland) model for the steric effect and the Born model for the electrostriction effect. Our model is an extension of the previous ones for electrolyte solutions[2] and for non-ionic ternary mixtures composed of a solute and a binary mixture solvent.[36] We have then numerically examined how K_{S} and C_{I} depend on the ion and solute sizes. Regarding K_{S}, our simple model semi-quantitatively reproduces the the experimental data. In particular, the inversion of solute size (α_{h}) dependence of K_{S} for large ions have been explained by the interplay of steric and electrostriction effects. The negative value of K_{S} observed for large ions and solutes, e.g., benzene and CsI in Table 1, is also reproduced as a result of the steric effects and short-range attractive interactions. For small ions and solutes, we have a rather simple expression $K_{\mathrm{S}} \approx K_{\mathrm{S}}^{\mathrm{el}} = -v_{\mathrm{h}}^* v_{\mathrm{I}}^{\mathrm{el}}/\kappa_{\mathrm{w}}$. While our simple model cannot reproduce the irregular behavior of Li$^+$, Eq. (52) suggests that the small K_{S} values associated with Li$^+$ are the result of the weak electrostriction effect on the partial volume of Li$^+$ as compared with that of Na$^+$.

The correlation between the salt effect on the solute solubility and that on the solute-solute effective interaction that has been known by earlier simulation studies has been accounted for by the explicit connection between K_{S} and C_{I} in Eqs. (40)–(42). When ions and solutes are not very large, we have the simple

quadratic relation $C_I \approx K_S^2/4$ in Eq. (58). The right hand side of Eq. (58) is the contribution from $-k_B T \chi_I g_h^2$ in Eq. (39), i.e., the coupling of composition fluctuations and the asymmetric solute-solvent interactions (see also Eq. (42)). This prediction is qualitatively consistent with the salt-induced downward shifts of solute-solute PMFs obtained from MD simulations of methane and neopentane in alkali-halide solutions.[31] Furthermore, we have confirmed that the data of the recent MD simulations of a methane-NaCl-water solution[33] satisfies Eq. (58). This approximate relation (58) is less precise for large ions and solutes, but can nevertheless be used for a rough estimate of C_I in the wide range of ion and solute sizes.

We make final remarks. (i) While our numerical calculations reproduce the overall behavior of the experimental data of K_S fairly well, our model free energy remains rather approximate; it takes into account neither the asymmetry between the cation-water and anion-water interactions nor the hydrogen-bonding between water molecules. The latter effect, for example, should play a relevant role in the temperature dependence of gas solubility in aqueous electrolyte solutions as in pure water.[54] (ii) Although we have seen that the relation Eq. (58) is in good agreement with the data of previous MD simulations in methane-NaCl-water, quantitative understanding of the correlation between K_S and C_I for non-polar solutes remains incomplete. MD simulations for various combinations of solutes and ions would be informative. (iii) It is known that for molecular species with both hydrophobic and hydrophilic groups such as alcohols, surfactants, peptides the Sechenov coefficient is relatively small (shift towards salting-in) as compared with non-polar ones.[15] Salt effects on the effective interactions between such solutes would also be interesting.[65]

Supporting Information Available

The following Supporting Information is available free of charge at the ACS website.

- Sec. SI-A: Inversion of I^{ij} for small n_h

- Sec. SI-B: Calculation of $C_I^{(1)}$

- Sec. SI-C: Expressions for salts of general valence numbers

- Sec. SI-D: Long-wavelength density fluctuations

- Sec. SI-E: Kirkwood-Buff integrals
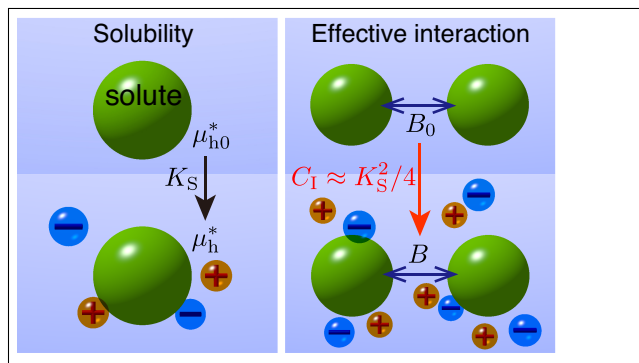
- Sec. SI-F: Debye-McAulay theory

References

(1) Robinson, R. A.; Stokes, R. H. *Electrolyte Solutions*; 2nd ed.; Dover: Mineola, NY, 2002.

(2) Okamoto, R.; Koga, K.; Onuki, A. Theory of electrolytes including steric, attractive, and hydration interactions. *J. Chem. Phys.* **2020**, *153*, 074503.

(3) Garrett, B. C. Ions at the air/water interface. *Science* **2004**, *303*, 1146–1147.

(4) Kunz, W.; Nostro, P. L.; Ninham, B. W. The present state of affairs with Hofmeister effects. *Curr. Opin. Coll. Int. Sci.* **2004**, *9*, 1–18.

(5) Jenkins, H. D. B.; Marcus, Y. Viscosity B-coefficients of ions in solution. *Chem. Rev.* **1995**, *95*, 2695–2724.

(6) Yurchenko, S. O.; Shkirin, A. V.; Ninham, B. W.; Sychev, A. A.; Babenko, V. A.; Penkov, N. V.; Kryuchkov, N. P.; Bunkin, N. F. Ion-Specific and Thermal Effects in the Stabilization of the Gas Nanobubble

Phase in Bulk Aqueous Electrolyte Solutions. *Langmuir* **2016**, *32*, 11245–11255.

(7) Okamoto, R.; Onuki, A. Precipitation in aqueous mixtures with addition of strongly hydrophilic or hydrophobic solute. *Phys. Rev. E* **2010**, *82*, 051501.

(8) Onuki, A.; Okamoto, R. Selective solvation effects in phase separation in aqueous mixtures. *Curr. Opin. Coll. Int. Sci.* **2011**, *16*, 525–533.

(9) Onuki, A.; Yabunaka, S.; Araki, T.; Okamoto, R. Structure formation due to antagonistic salts. *Curr. Opin. Coll. Int. Sci.* **2016**, *22*, 59–64.

(10) Sadakane, K.; Onuki, A.; Nishida, K.; Koizumi, S.; Seto, H. Multilamellar structures induced by hydrophilic and hydrophobic ions added to a binary mixture of DO and 3-methylpyridine. *Phys. Rev. Lett.* **2009**, *103*, 167803.

(11) Kunz, W.; Henle, J.; Ninham, B. W. Zur Lehre von der Wirkung der Salz. *Curr. Opin. Coll. Int. Sci.* **2004**, *9*, 19–37.

(12) Nostro, P. L.; Ninham, B. W. Hofmeister phenomena: an update on ion specificity in biology. *Chem. Rev.* **2012**, *112*, 2286–2322.

(13) Jungwirth, P.; Cremer, P. S. Beyond Hofmeister. *Nature Chem.* **2014**, *6*, 261–263.

(14) Setschenow, J. J. Über die Konstitution der Salzlösungen auf Grund ihres Verhaltens zu Kohlensäure. *Z. Phys. Chem.* **1889**, *4*, 117–125.

(15) Long, F. A.; McDevit, W. F. Activity Coefficients of Nonelectrolyte Solutes in Aqueous Salt Solutions. *Chem. Rev.* **1952**, *51*, 119–169.

(16) Clever, H. L. Setchenov Salt-Effect Parameter. *J. Chem. Eng. Data* **1983**, *28*, 340–343.

(17) Schumpe, A. The Estimation of Gas Solubilities in Salt Solutions. *Chem. Eng. Sci.* **1993**, *48*, 153–158.

(18) Hermann, C.; Dewes, I.; Schumpe, A. The Estimation of Gas Solubilities in Salt Solutions. *Chem. Eng. Sci.* **1995**, *50*, 1673–1675.

(19) Weisenberger, S.; Schumpe, A. Estimation of Gas Solubilities in Salt Solutions at Temperatures from 273 K to 363 K. *AIChE J.* **1996**, *42*, 298–300.

(20) Smith, P. E. Computer simulation of cosolvent effects on hydrophobic hydration. *J. Phys. Chem. B* **1999**, *103*, 525–534.

(21) Docherty, H.; Galindo, A.; Sanz, E.; Vega, C. Investigation of the Salting Out of Methane from Aqueous Electrolyte Solutions Using Computer Simulations. *J. Phys. Chem. B* **2007**, *111*, 8993–9000.

(22) Ganguly, P.; Hajari, T.; van der Vegt, N. F. A. Molecular Simulation Study on Hofmeister Cations and the Aqueous Solubility of Benzene. *J. Phys. Chem. B* **2014**, *118*, 5331–5339.

(23) Katsuto, H.; Okamoto, R.; Sumi, T.; Koga, K. Ion Size Dependences of the Salting-Out Effect: Reversed Order of Sodium and Lithium Ions. *J. Phys. Chem. B* **2021**, *125*, 6296–6305.

(24) Kinoshita, M.; Hirata, F. Analysis of Salt Effects on Solubility of Noble Gases in Water Using the Reference Interaction Site Model Theory. *The Journal of Chemical Physics* **1997**, *106*, 5202–5215.

(25) Hribar, B.; Southall, N. T.; Vlachy, V.; Dill, K. A. How Ions Affect the Structure of Water. *J. Am. Chem. Soc.* **2002**, *124*, 12302–12311.

(26) Debye, P.; McAulay, J. Das Elektrische Feld Der Ionen Und Die Neutralsalzwirking (The electric field of ions and the action of neutral salts). *Physik. Z.* **1925**, *26*, 22–29.

(27) Ghosh, T.; García, A. E.; Garde, S. Water-Mediated Three-Particle Interactions between Hydrophobic Solutes: Size, Pressure, and Salt Effects. *J. Phys. Chem. B* **2003**, *107*, 612–617.

(28) Ghosh, T.; Kalra, A.; Garde, S. On the Salt-Induced Stabilization of Pair and Many-Body Hydrophobic Interactions. *J. Phys. Chem. B* **2005**, *109*, 642–651.

(29) Fujita, T.; Watanabe, H.; Tanaka, S. Effects of Salt Addition on Strength and Dynamics of Hydrophobic Interactions. *Chem. Phys. Lett.* **2007**, *434*, 42–48.

(30) Jönsson, M.; Skepö, M.; Linse, P. Monte Carlo Simulations of the Hydrophobic Effect in Aqueous Electrolyte Solutions. *J. Phys. Chem. B* **2006**, *110*, 8782–8788.

(31) Thomas, A. S.; Elcock, A. H. Molecular Dynamics Simulations of Hydrophobic Associations in Aqueous Salt Solutions Indicate a Connection between Water Hydrogen Bonding and the Hofmeister Effect. *J. Am. Chem. Soc.* **2007**, *129*, 14887–14898.

(32) Kirkwood, J. G.; Buff, F. P. The statistical mechanical theory of solutions. I. *J. Chem. Phys.* **1951**, *19*, 774–777.

(33) Koga, K.; Yamamoto, N. Hydrophobicity Varying with Temperature, Pressure, and Salt Concentration. *J. Phys. Chem. B* **2018**, *122*, 3655–3665.

(34) Koga, K.; Holten, V.; Widom, B. Deriving second osmotic virial coefficients from equations of state and from experiment. *J. Phys. Chem. B* **2015**, *119*, 13391–13397.

(35) Cerdeiriña, C. A.; Widom, B. Osmotic second virial coefficients of aqueous solutions from two component equations of state. *J. Phys. Chem. B* **2016**, *120*, 13144–13151.

(36) Okamoto, R.; Onuki, A. Theory of nonionic hydrophobic solutes in mixture solvent: Solvent-mediated interaction and solute-induced phase separation. *J. Chem. Phys.* **2018**, *149*, 014501.

(37) Boublík, T. Hard-Sphere Equation of State. *J. Chem. Phys.* **1970**, *53*, 471–472.

(38) Mansoori, G. A.; Carnahan, N. F.; Starling, K. E.; Leland, T. W. Equilibrium thermodynamic properties of the mixture of hard spheres. *J. Chem. Phys.* **1971**, *54*, 1523–1525.

(39) Born, M. Volumen und hydratationswärme der Ionen (Volume and hydration heat of ions). *Z. Physik* **1920**, *1*, 45–48.

(40) Weerasinghe, S.; Smith, P. E. A Kirkwood-Buff derived force field for sodium chloride in water. *J. Chem. Phys.* **2003**, *119*, 11342–11349.

(41) Kalcher, I.; Dzubiella, J. Structure-thermodynamics relation of electrolyte solutions. *J. Chem. Phys.* **2009**, *130*, 134507.

(42) Klasczyk, B.; Knecht, V. Kirkwood-Buff derived force field for alkali chlorides in simple point charge water. *J. Chem. Phys.* **2010**, *132*, 024109.

(43) Fyta, M.; Netz, R. R. Ionic force field optimization based on single-ion and ion-pair solvation properties: Going beyond standard mixing rules. *J. Chem. Phys.* **2012**, *136*, 124103.

(44) Shimizu, S.; McLaren, W. M.; Matubayasi, N. The Hofmeister Series and Protein-Salt Interactions. *J. Chem. Phys.* **2006**, *124*, 234905.

(45) Ben-Naim, A. *Molecular theory of solutions*; Oxford, 2006.

(46) Smith, P. E.; Mazo, R. M. On the Theory of Solute Solubility in Mixed Solvents. *J. Phys. Chem. B* **2008**, *112*, 7875–7884.

(47) Millero, F. J. The molal volumes of electrolytes. *Chem. Rev.* **1971**, *71*, 147–176.

(48) Mazzini, V.; Craig, V. S. J. What is the fundamental ion-specific series for anions

and cations? Ion specificity in standard partial molar volumes of electrolytes and electrostriction in water and non-aqueous solvents. *Chem. Sci.* **2017**, *8*, 7052–7065.

(49) Zana, R.; Yeager, E. Ultrasonic Vibration Potentials and Their Use in the Determination of Ionic Partial Molal Volumes. *The Journal of Physical Chemistry* **1967**, *71*, 521–536.

(50) Talanquer, V.; Cunningham, C.; Oxtoby, D. W. Bubble nucleation in binary mixtures: A semiempirical approach. *J. Chem. Phys.* **2001**, *114*, 6759–6762.

(51) Weeks, J. D.; Chandler, D.; Andersen, H. C. Role of repulsive forces in determining the equilibrium structure of simple liquids. *J. Chem. Phys.* **1971**, *54*, 5237–5247.

(52) Okamoto, R.; Onuki, A. Density functional theory of gas-liquid phase separation in dilute binary mixtures. *J. Phys.: Condens. Matter* **2016**, *28*, 244012.

(53) Poole, P. H.; Sciortino, F.; Grande, T.; Stanley, H. E.; Angell, C. A. Effect of Hydrogen Bonds on the Thermodynamic Behavior of Liquid Water. *Phys. Rev. Lett.* **1994**, *73*, 1632–1635.

(54) Cerdeiriña, C. A.; Debenedetti, P. G. Water Anomalous Thermodynamics, Attraction, Repulsion, and Hydrophobic Hydration. *J. Chem. Phys.* **2016**, *144*, 164501.

(55) Oster, G. The Dielectric Properties of Liquid Mixtures. *J. Am. Chem. Soc.* **1946**, *68*, 2036–2041.

(56) Harvey, A. H.; Prausnitz, J. M. Dielectric Constants of Fluid Mixtures over a Wide Range of Temperature and Density. *Journal of Solution Chemistry* **1987**, *16*, 857–869.

(57) Debye, P.; Hückel, E. Zur theorie der elektrolyte. I. Gefrierpunktserniedrigung und verwandte erscheinungen (The theory of electrolytes. I. Lowering of freezing point and related phenomena). *Phys. Z.* **1923**, *24*, 185–206.

(58) Archer, D. G.; Wang, P. The dielectric constant of water and Debye Hückel limiting law slopes. *J. Phys. Chem. Ref. Data* **1990**, *19*, 371–411.

(59) Fernández, D. P.; Goodwin, A. R. H.; Lemmon, E. W.; Sengers, J. M. H. L.; Williams, R. C. ions. *J. Phys. Chem. Ref. Data* **1997**, *26*, 1125–1166.

(60) Fine, R. A.; Millero, F. J. Compressibility of water as a function of temperature and pressure. *J. Chem. Phys.* **1973**, *59*, 5529–5536.

(61) Collins, K. D. Charge density-dependent strength of hydration and biological structure. *Biophys. J.* **1997**, *72*, 65–76.

(62) Hepler, L. G. PARTIAL MOLAL VOLUMES OF AQUEOUS IONS. *J. Phys. Chem.* **1957**, *61*, 1426–1428.

(63) Marcus, Y. Electrostriction in Electrolyte Solutions. *Chem. Rev.* **2011**, *111*, 2761–2783.

(64) Drude, P.; Nernst, W. On the electrostriction induced by free ions. *Z. Phys. Chem.* **1894**, *15*, 79–85.

(65) Mendes de Oliveira, D.; Ben-Amotz, D. Spectroscopically Quantifying the Influence of Salts on Nonionic Surfactant Chemical Potentials and Micelle Formation. *J. Phys. Chem. Lett.* **2021**, *12*, 355–360.

Graphical TOC Entry

TOC Graphic